Thermal Performance of Additively Manufactured Three-dimensional Oscillating Heat Pipe with Check Valves in Various Orientations

Makiko Ando[1] and Atsushi Okamoto[2]
Japan Aerospace Exploration Agency (JAXA), Tsukuba, Ibaraki, 305-8505, Japan

An oscillating heat pipe (OHP) is an attractive thermal control device with high heat transport capability and is best suited to heat transfer in a narrow space. The Japan Aerospace Exploration Agency (JAXA) has developed an OHP with check valves (CVOHP) for space applications. CVOHPs are assumed to be used in three-dimensional shapes such as an L shape, a U shape, or more complex ones. Recently, metal additive manufacturing has been focused as a promising solution to fabricating CVOHPs with complex three-dimensional shapes. In this study, we evaluated the thermal performance of an additively manufactured CVOHP (AM-CVOHP) with a U shape in various orientations: horizontal, bottom heat, top heat, concave, and convex orientations. The test results showed that the AM-CVOHP operated stably at all orientations except for the top heat orientation. In the horizontal, bottom heat, and concave orientations, the AM-CVOHP could transport up to 200 W of heat with an effective thermal conductivity of 3000 to 7000 W/mK. The maximum heat transport in the top heat orientation was 100 W, and the effective thermal conductivity was lower than in the other orientations. Also, startup failure was observed when the AM-CVOHP was heated after being kept at the top heat orientation over a certain time. As described above, the U-shaped AM-CVOHP operated well in most orientations except for top heat and convex orientations. Further investigation is needed to develop orientation-independent three-dimensional CVOHPs.

Nomenclature

A	=	cross-sectional area
Bo	=	Bond number
D	=	inner diameter
g	=	gravitational acceleration
L	=	heat transfer distance
Q_{net}	=	net heat transport
$T_{e,\,avg}$	=	average temperature of the evaporator section
$T_{c,\,avg}$	=	average temperature of the condenser section
λ_{eff}	=	effective thermal conductivity
ρ_l	=	liquid density
ρ_v	=	vapor density
σ	=	surface tension

I. Introduction

AN oscillating heat pipe (OHP), also known as a pulsating heat pipe (PHP), is an attractive thermal control device with high heat transport capability due to sensible and latent heat use. It also enables heat transfer within narrow spaces because it consists only of a meandering capillary tube and working fluid. Thus, an OHP is a promising device

[1] Associate Senior Researcher, Research Unit II, Research and Development Directorate, 2-1-1 Sengen, Tsukuba, Ibaraki, Japan.
[2] Manager for Thermal Division, Research Unit II, Research and Development Directorate, 2-1-1 Sengen, Tsukuba, Ibaraki, Japan.

for removing heat from a heat source inside a component and from high-density mounted components in spacecraft. During the last decade, several researchers have performed short-term microgravity and long-term on-orbit experiments on OHPs for future space applications. The OHPs showed no significant difference in thermal performance between microgravity experiments and horizontal orientation on the ground[1-4].

Figure 1 (a) shows a typical closed-loop OHP. A train of liquid slugs and vapor bubbles exists in the flow channel. The OHP is usually divided into three sections: evaporator, adiabatic, and condenser sections. The flow channel goes back and forth between the evaporator and condenser sections many times. When heat is applied to the evaporator section, boiling and expansion of vapor bubbles occur. Conversely, the vapor bubbles contract and condense in the condenser section. The expansion and contraction of vapor bubbles cause a pressure difference between the evaporator and condenser sections, which creates an oscillating or circulating motion of the working fluid. This is the basic operating principle of OHPs.

The Japan Aerospace Exploration Agency (JAXA) has developed an OHP with check valves (CVOHP), as shown in Figure 1 (b). The CVOHP was first suggested by Miyazaki et al.[5], aiming to improve thermal conductance and extend operational limits. The key point for the high thermal performance of an OHP is to supply liquid continuously to the evaporator section. The check valves enable that by making fluid flow unidirectional rather than oscillatory. Several researchers studied CVOHPs with several types of check valves, such as the floating-type[5-6], Tesla-type[7-9], spring-loaded type[10], and hook-shaped type[11]. Those studies showed that the CVOHP enhanced the thermal conductance by several tens of percent. JAXA has performed the on-orbit experiment of the CVOHP with floating-type check valves from 2012 to 2016[4]. The CVOHP was a meandering stainless-steel tube sandwiched between aluminum alloy plates, and the on-orbit experiment showed that the CVOHP had an effective thermal conductivity of approximately 6000 W/mK, more than 30 times that of standard aluminum alloy.

We are now working toward practical applications of CVOHPs. One practical use is employing the CVOHP in a three-dimensional structure, such as an L shape, a U shape, or a more complex one. However, tube-based OHPs have difficulty being shaped into complex three-dimensional configurations. In recent years, additive manufacturing (AM) has become attractive as a fabrication method for OHPs. Several researchers have studied flat-plate or three-dimensional OHPs fabricated by metal AM[12-15]. In our previous study, we succeeded in fabricating a flat-plate and a U-shaped AM-CVOHP and evaluated the thermal performance only in horizontal orientation[16]. This paper describes thermal performance tests of the U-shaped AM-CVOHP in various orientations: horizontal, bottom heat, top heat, concave, and convex.

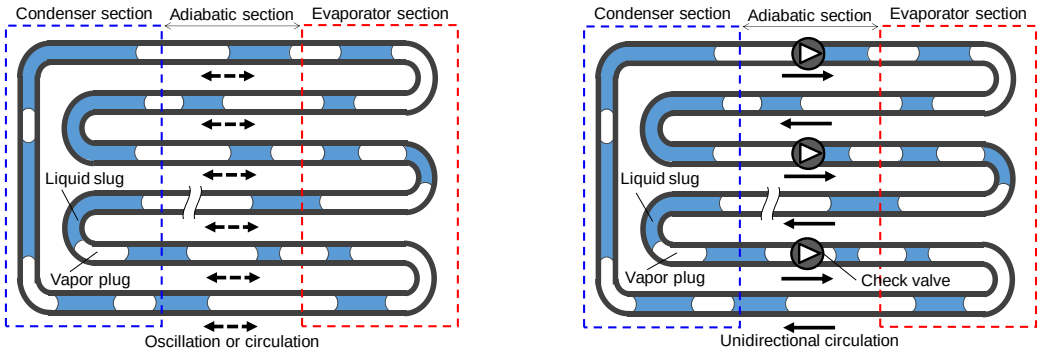

(a) Closed-loop OHP (b) CVOHP

Figure 1. Schematic of closed-loop OHP and CVOHP.

II. Design and Fabrication of U-shaped AM-CVOHP

Figure 2 shows a schematic view of the U-shaped AM-CVOHP. It has 20 parallel channels (i.e., ten turns), and the flow channel has a circular cross-section with an inner diameter of about 1 mm. Inner diameter of an OHP is commonly selected based on the threshold shown in Eq. (1).

$$Bo = \frac{g(\rho_l - \rho_v)D^2}{\sigma} \leq 4 \quad (1)$$

Bo is Bond number, g is gravitational acceleration, ρ_l is liquid density, ρ_v is vapor density, D is inner diameter, and σ is surface tension. As described in Section III, HFC-134a was used as working fluid in this study. The inner diameter of 1 mm satisfies Eq. (1) for HFC-134a below 75 °C. The plate is 3 mm thick. A floating-type check valve is employed in the adiabatic section for each turn, allowing the flow from the condenser to the evaporator section. The design of the check valve is also shown in Figure 2. The check valve consists of a ceramic ball, a conical valve seat, and a ball stopper. The ball stopper is a simple rod standing at the center of the cross-section. The major specifications of the AM-CVOHP are listed in Table 1.

The AM-CVOHP was additively manufactured using AlSi10Mg powders by selective laser melting (SLM) in a powder bed. When manufacturing the check valve, the process was stopped and restarted to allow a ceramic ball to be inserted. In fabricating structures with internal capillary channels, removing residual powders is essential. Removing powders in making an AM-CVOHP is more difficult due to the narrow flow path in the check valves. A venting port was created for each turn for powder removal, as shown in Figure 2. The powder was removed by blowing air thorough the device and exposing it to vibration. The venting ports were sealed after powder removal by adding metal layers over them. Figure 3 is an external view of the AM-CVOHP and an X-ray transmission image of the adiabatic section. The flow channel, including check valves, was fabricated as expected without clogging. A ball valve was installed at the charging port in the condenser section to charge the working fluid. The mass of the AM-CVOHP is estimated to be about 10 % lighter than a similar CVOHP manufactured by the conventional method using stainless steel tube and aluminum plates.

III. Thermal Performance Test Conditions

The thermal performance tests of the U-shaped AM-CVOHP were performed. Figure 4 shows a schematic of the basic setup. The condenser section was mounted on the cold plate. The temperature of the cold plate was kept at the

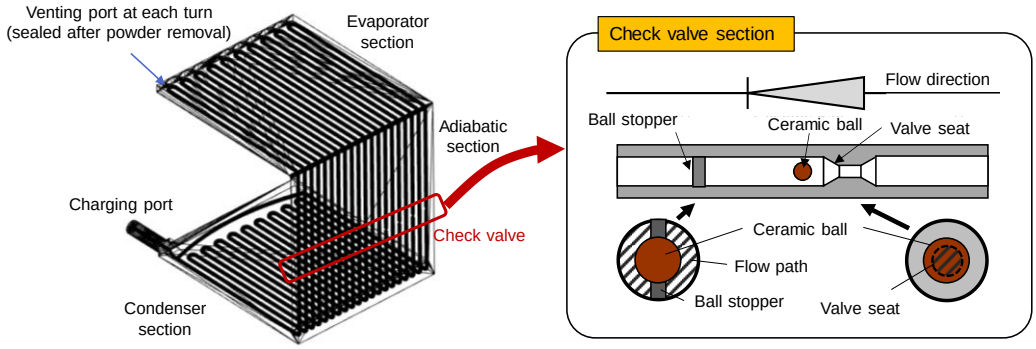

Figure 2. Schematic and external view of U-shaped AM-CVOHP.

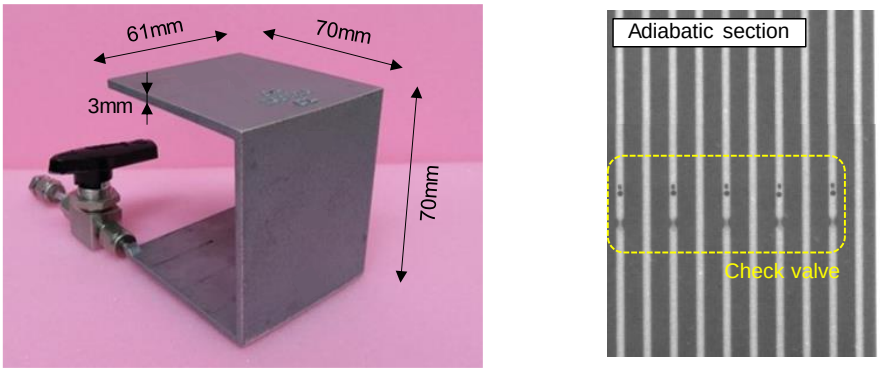

(a) External view (b) X-ray transmission image

Figure 3. External view and X-ray transmission image of the AM-CVOHP.

Table 1 Major specifications of the U-shaped AM-CVOHP.

Dimension	70 mm × 70 mm × 61 mm (excluding charging port)
Plate thickness	3 mm
Plate material	AlSi10Mg
Channel diameter	1 mm
Number of turns	10
Length of each section	70 mm for evaporator/adiabatic/condenser section
Check valve layout	Floating-type check valve at adiabatic section for each turn

Table 2 Experimental uncertainties.

Instrument	Range	Uncertainty
DC power supply (TEXIO PSW-360M250)	Voltage: 0 to 250 V Current: 0 to 4.5 A	Voltage: ±2% of rdg. (analog monitor) Current: ±2% of rdg. (analog monitor)
Data logger (YOKOGAWA MX100)	Thermocouple: -200 to 400 ℃ Voltage: 0 to 6 V	Thermocouple: ±(0.05% of rdg. + 0.5 ℃) Voltage: ±(0.05% of rdg. + 0.2 mV)
T-type thermocouple	-200 to 400 ℃	±1.0 ℃

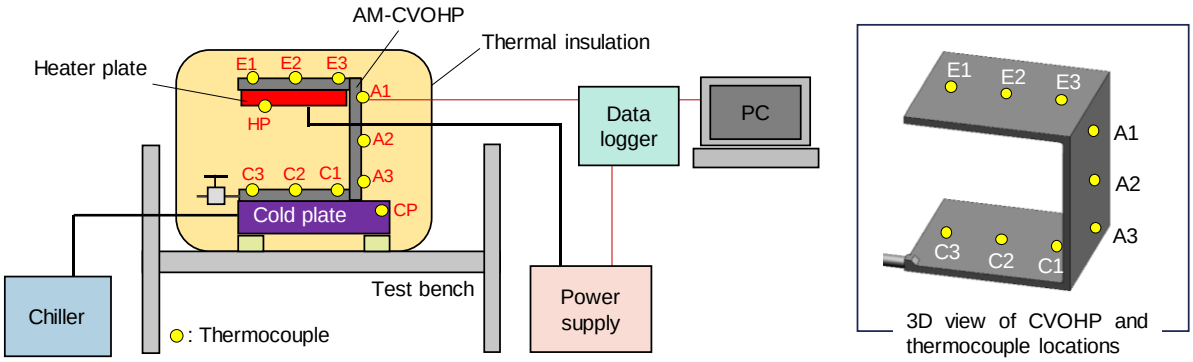

Figure 4. Thermal performance test setup of U-shaped AM-CVOHP. *Yellow circles and red letters show the temperature measurement points and their names.*

set temperature using a chiller. The heater plate was attached to the evaporator section. During the test, the AM-CVOHP, the cold plate, and the heater plate were covered with insulating material to suppress heat leaks to the surroundings. Temperature measurement points are shown by yellow circles in Figure 4. Three T-type thermocouples were attached to each of the evaporator (E1–E3), adiabatic (A1–A3), and condenser (C1–C3) sections. The temperature of the heater plate and cold plate were also measured. The tests were performed in six different orientations as shown in Figure 5: horizontal-1, horizontal-2, top heat, bottom heat, concave, and convex. Table 2 lists the experimental uncertainties.

As for Figure 5 (a) and (b), the AM-CVOHP was installed horizontally. “Horizontal” indicates that there is no height difference between the evaporator and condenser sections in the same turn. The difference between horizontal-1 and -2 is the relationship between the direction of circulating flow and that of gravity. In horizontal-1, the circulating direction in the return path of the condenser section and the direction of gravity coincide, and vice versa in horizontal-2. In top heat (Figure 5 (c)), the evaporator was positioned above the condenser, and vice versa in bottom heat (Figure 5 (d)). The concave and convex orientations (Figure 5 (e) and (f)) are specific to the U-shape. As for the concave orientation, the adiabatic section is positioned horizontally at the bottom, and the condenser and evaporator sections are positioned vertically. The adiabatic section is positioned horizontally at the top in the convex orientation.

The test conditions are listed in Table 3. HFC-134a was charged in the AM-CVOHP at a filling ratio of 47 wt%. HFC-134a is particularly well suited as OHP working fluid in a view of minimal startup heat flux and large heat transport capability[17]. After the cold plate was set to 10 ℃, the heat was input to the evaporator section by the heater plate, and the steady-state temperature data was obtained. The heat input was 20 W at the minimum and was increased in 20 W increments until the AM-CVOHP stopped working. The tests were repeated twice for each orientation to confirm reproducibility.

IV. Results and Discussion

Figure 6 shows examples of the temperature history of the U-shaped AM-CVOHP, a heater plate, and a cold plate for several orientations: horizontal-1, top heat, bottom heat, and convex. The average thermocouple readings are the plots for the evaporator, adiabatic, and condenser sections of the AM-CVOHP.

In the horizontal-1 and bottom heat cases (Figure 6 (a) and (c)), the CVOHP started up smoothly when 20 W was applied. Temperature oscillations were very small at each heat input, indicating that the CVOHP operated quite stably. In these two cases, the CVOHP operated well up to 220 W. Then it stopped operating at 240 W with a sharp increase in the evaporator temperature due to dryout. For the convex case (Figure 6 (d)), the temperature remained relatively stable, but a slight oscillation of the evaporator temperature was observed at 120 W. The dryout heat input was 200 W, slightly lower than the previous two cases.

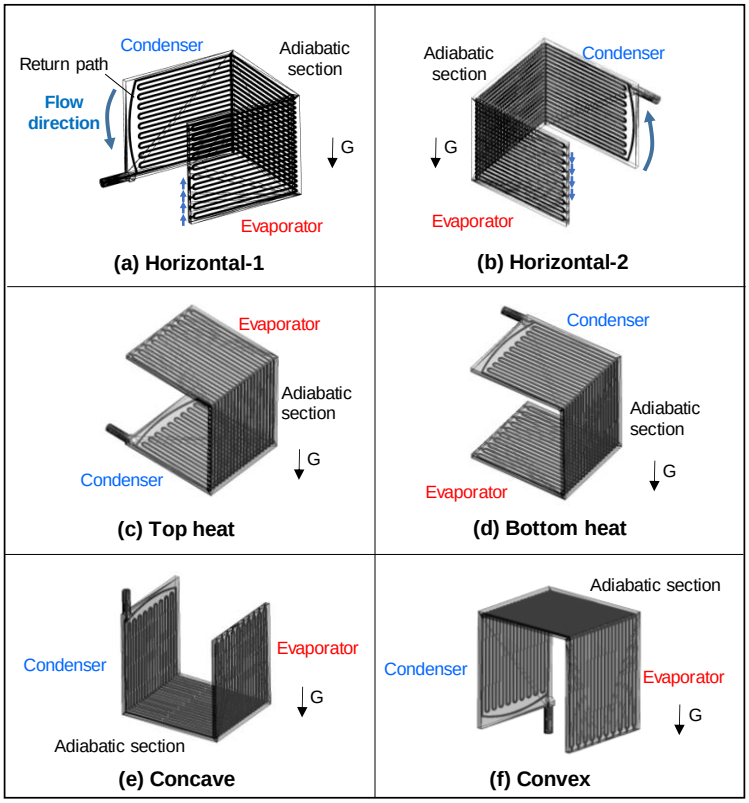

Figure 5. Definitions U-shaped AM-CVOHP orientation.

Table 3 Test conditions.

Working fluid / Filling ratio	HFC-134a, 47 wt%
Orientation	Horizontal-1, -2 Top heat, Bottom heat Concave, Convex
Cold plate temperature	10 ℃
Heat input	From 20 W until the AM-CVOHP stops working

Conversely, in the top heat case (Figure 6 (b)), the CVOHP did not start up even after 20 W was applied. The temperature increase of the heater plate and the evaporator section from the elapsed time of 1:00 indicates startup failure. After ten minutes had passed, a recovery operation was performed to make the CVOHP start up. The orientation of the CVOHP was temporarily changed to horizontal-1. Then, the CVOHP was returned to the top heat orientation, and steady-state data were acquired from 20 W as planned. The fact that the temporal orientation change worked well to make the CVOHP start up indicates that liquid localized in the condenser section. The top heat test was performed after the previous day's CVOHP was installed in that orientation. Consequently, the liquid was localized to the condenser section due to the gravitational effect, causing insufficient liquid in the evaporator section and startup failure. After the recovery operation for startup, the CVOHP operated stably up to 80 W in top heat orientation. However, the evaporator temperature oscillated significantly at 100 W, and the CVOHP stopped working at 120 W.

From the steady-state data at each heat input, the thermal performance was evaluated in terms of effective thermal conductivity λ_{eff}, expressed by Eq. (2).

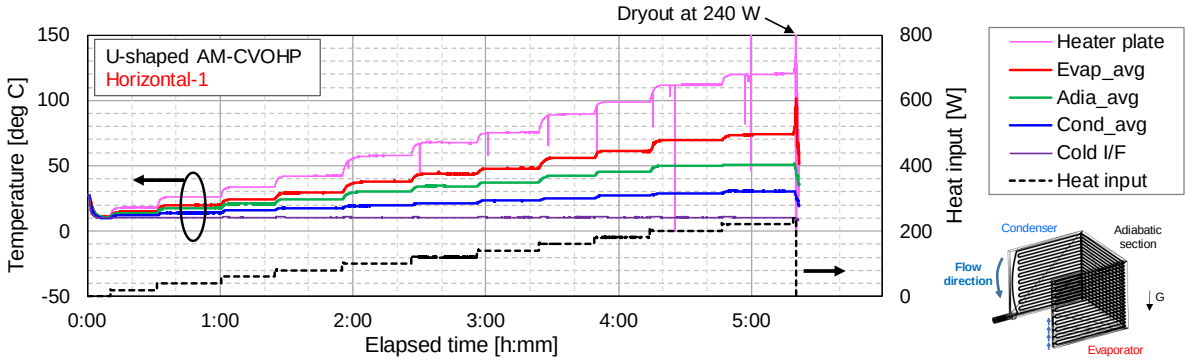

(a) Horizontai-1

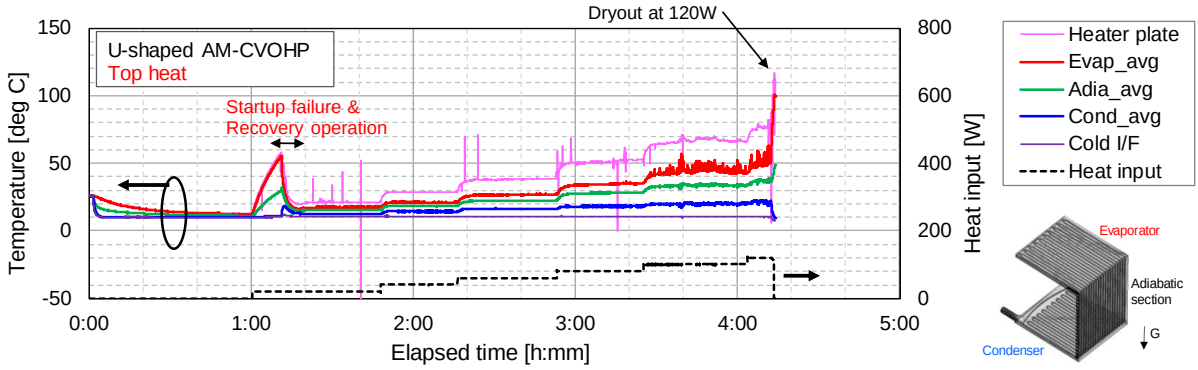

(b) Top heat

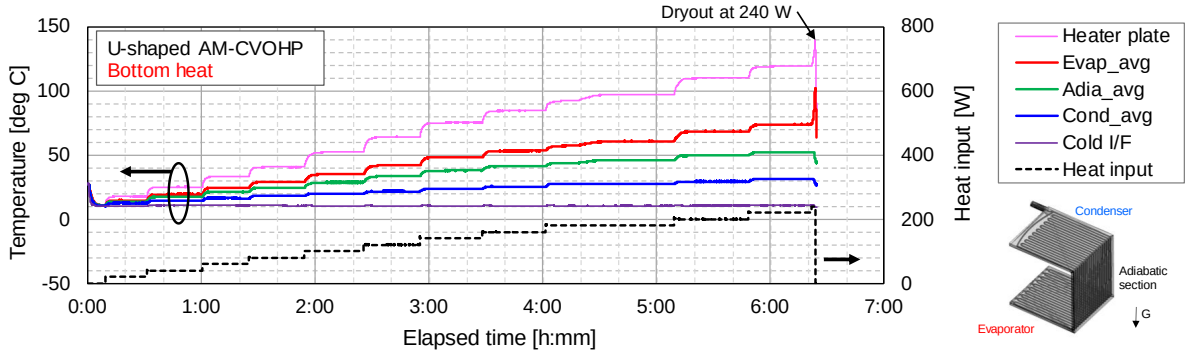

(c) Bottom heat

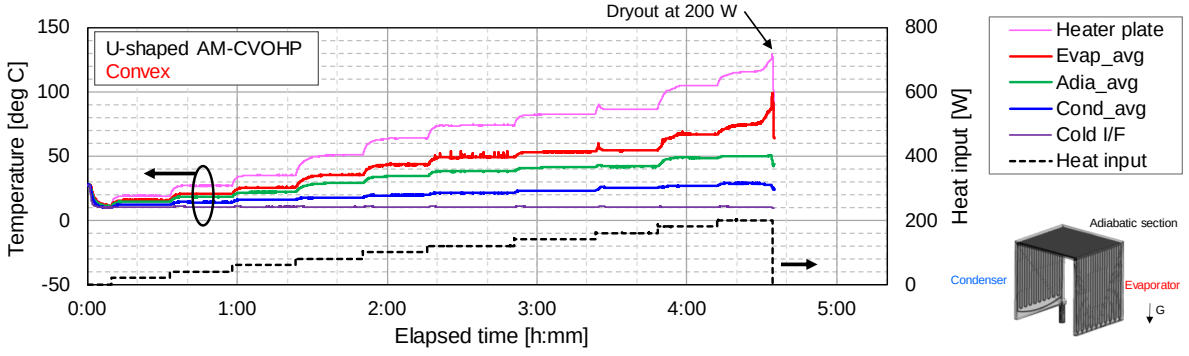

(d) Convex

Figure 6. Temperature history for horizontal-1, top heat, bottom heat, and convex orientations.

$$\lambda_{eff} = \frac{Q_{net}}{T_{e,avg} - T_{c,avg}} \frac{L}{A} \tag{2}$$

Q_{net} is the net heat transport of the CVOHP, which is calculated by subtracting the heat leaking to the surroundings from the heat input. $T_{e,avg}$ and $T_{c,avg}$ are temperatures of the evaporator and condenser sections, respectively, averaged over 3 min. in the steady-state. L is the heat transport distance, the distance between the center of the evaporator section and the center of the condenser section. A is the cross-sectional area of the CVOHP.

Figure 7 shows the effective thermal conductivity plotted against the net heat transport for the different orientations. The effect of orientation on the effective thermal conductivity is significant at lower heat input. The trends of effective thermal conductivity are similar except for the top heat and convex cases. The effective thermal conductivity was around 3000 to 7000 W/mK, which is 26 to 60 times as high as the thermal conductivity of the AM wall (117 W/mK). The top heat and convex cases have similar trends below 100 W, with the effective thermal conductivity decreasing as the heat input increases toward 100 W. On the other hand, it is interesting to note that the CVOHP stopped operating above 100 W in the top heat case, whereas the CVOHP did not dryout and the performance recovered in the convex case.

Maximum heat transport is shown in Figure 8. This study defines maximum heat transport as the net heat transport just before the CVOHP stopped operating. The maximum heat transport of horizontal-1 was comparable to that of bottom heat. The thermal performance of horizontal-2 was expected to be less favorable than horizontal-1 because gravity would interfere with the long liquid column's circulation through the condenser section's return path. However, the test results showed that the difference between horizontal-1 and -2 was slight for the CVOHP with 10 turns. As the number of turns increases, the length of the condenser section's return path also increases. As a result, the liquid column moves against gravity over a longer distance, and the obstruction of the circulation flow is expected to be more pronounced than when the number of turns is small. In the concave case, gravity could affect the fluid motion in the evaporator and condenser section, but no significant effect was observed on the maximum heat transport. The convex case showed a similar trend to the top heat case up to 100 W, but it recovered and finally transported heat up to 170 W. In the top heat case, the maximum heat transport dropped significantly to half the others.

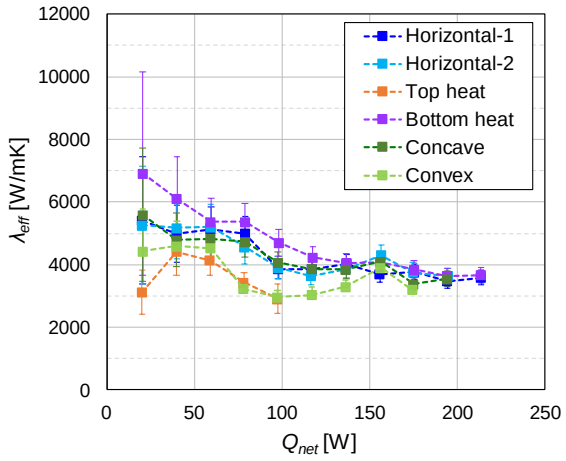

Figure 7. Effective thermal conductivity.

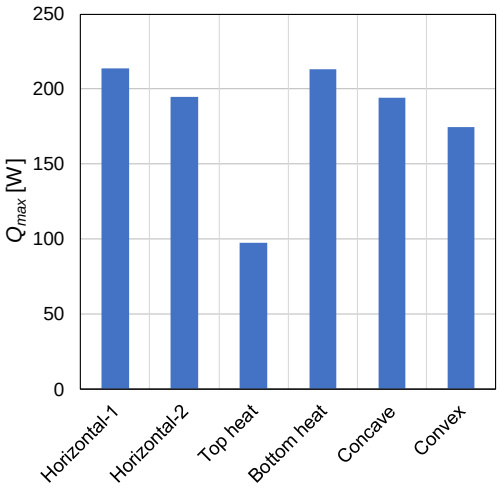

Figure 8. Maximum heat transport.

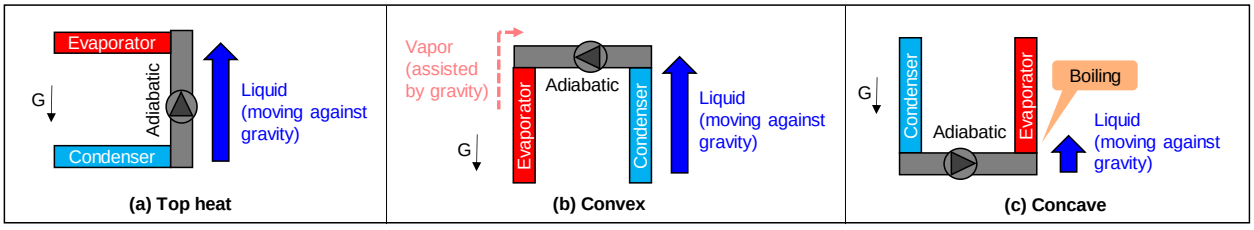

Figure 9. Gravitational effect on each section of the CVOHP for top heat, convex and concave orientations.

Thermal performance test results showed that the CVOHP operated well in the horizontal-1, -2, bottom heat, and concave orientations, while the thermal performance decreased in the top heat and convex orientations. The fluid behavior is discussed here for the latter two orientations. Figure 9 briefly shows the gravitational effect on each section of the CVOHP for top heat and convex orientations. The concave case is also shown for comparison. In the top heat case, there is no gravitational effect in the evaporator and condenser sections as shown in Figure 9 (a). However, gravity interferes with the liquid motion from the condenser to the evaporator section in the adiabatic section. Then, liquid supply to the evaporator section is weakened, decreasing effective thermal conductivity and dryout at relatively low heat input. Additionally, when the CVOHP was kept at top heat orientation over a certain time, startup failure would occur because of liquid localization in the condenser section caused by gravity.

Figure 9 (b) shows that the convex orientation is partially similar to the top heat in that gravity interferes with the liquid moving toward the evaporator section. This might be the main reason why the trend of effective thermal conductivity was similar to the top heat case up to moderate heat input. On the other hand, since the evaporator section is vertical, the vapor generated in the evaporator section can easily escape to the adiabatic section, which may enhance the circulation of the working fluid. At higher heat input, boiling occurs more actively, and the generated vapor can strongly push the neighboring liquid, enhancing the working fluid's circulation. This may be one of the reasons why the effective thermal conductivity recovered at higher heat input for the convex orientation. Figure 9 (c) shows the concave case for comparison. In the concave orientation, the liquid flow from the condenser to the adiabatic section is assisted by gravity, while the adiabatic section is not affected by gravity. Although the liquid flowing into the evaporator is against gravity, once the liquid reaches the inlet of the evaporator section, a pressure increase due to boiling strongly accelerates the liquid. As a result, a negative effect due to gravity is not significant for the concave case.

Thus, three-dimensional CVOHPs can be possibly used in various orientations. Although the gravitational effect is negligible on orbit, the difference in operating characteristics depending on orientation should be considered when performing ground tests. The thermal performance test results indicated that when the U-shaped CVOHP is installed in the top heat and convex orientations, it behaves differently from the expected on-orbit characteristics. Further investigation is needed to develop orientation-independent three-dimensional CVOHPs.

V. Conclusion

This study shows the thermal performance of the additively manufactured U-shaped CVOHP (AM-CVOHP) in various orientations: horizontal, bottom heat, top heat, concave, and convex. This evaluation is helpful to use CVOHPs effectively during the entire period, from ground tests to on-orbit. In horizontal, bottom heat, and concave orientations, the AM-CVOHP could transport heat up to 200 W, and its effective thermal conductivity was in the range from 3000 to 7000 W/mK. The thermal performance of the AM-CVOHP became lower in top heat orientation, and startup failure was observed when the AM-CVOHP was heated after being kept at the top heat orientation over a certain time. Additionally, the convex orientation showed a slightly lower thermal performance than horizontal, bottom heat, and concave orientations. The results indicated that the U-shaped AM-CVOHP showed lower thermal performance when gravity prevents liquid motion toward the evaporator. Further investigation is needed to develop orientation-independent three-dimensional CVOHPs.

References

[1]Ayel V., Araneo, L., Scalambra, A., Mameli, M., Romestant, C., Piteau, A., Marengo, M., Filippeschi, S., and Bertin, Y., "Experimental study of a closed loop flat plate pulsating heat pipe under a varying gravity force," *International Journal of Thermal Sciences*, Vol. 96, 2015, pp. 23-34.

[2]Mameli, M., Catarsi, A., Mangini, D., Pietrasanta, L., Miche, N., Marengo, M., Marco, P. D., and Filippeschi, S., "Start-up in microgravity and local thermodynamic states of a hybrid loop thermosyphon/pulsating heat pipe," *Applied Thermal Engineering*, Vol. 158, 2019, 113771.

[3]Drolen, B. L., Wilson C. A., Taft, B. S., Allison, J., and Irick, K. W., "Advanced Structurally Embedded Thermal Spreader Oscillating Heat Pipe Micro-Gravity Flight Experiment," *Journal of Thermophysics and Heat Transfer*, Vol. 36, No. 2, 2022, pp. 314-327.

[4]Ando, M., Okamoto, A., Tanaka, K., Maeda, M., Sugita, H., Daimaru, T., and Nagai, H., "On-orbit demonstration of oscillating heat pipe with check valves for space application," *Applied Thermal Engineering*, Vol. 130, 2018, pp. 552-560.

[5]Miyazaki, Y., Polasek, H., and Akachi, H., "Oscillating heat pipe with check valves," *Proceedings of 6th International Heat Pipe Symposium*, Chiang Mai, 2000.

[6]Rittidech, S., Pipatpaiboon, N., and Thongdaeng, S., "Thermal performance of horizontal closed-loop oscillating heat-pipe with check valves," *Journal of Mechanical Science and Technology*, Vol. 24, No. 2, 2010, pp. 545-550.

[7]Thompson, S. M., Ma, H. B., and Wilson, C., "Investigation of a flat-plate oscillating heat pipe with Tesla-type check valves," *Experimental Thermal and Fluid Science,* Vol. 35, 2011, pp. 1265-1273.

[8]de Vries, S. F., Florea, D., Homburg, F. G. A., and Frijns, A. J. H., "Design and operation of a Tesla-type valve for pulsating heat pipes," *International Journal of Heat and Mass Transfer*, Vol. 105, 2017, pp. 1-11.

[9]Wits, W. W., Groeneveld, G., and van Gerner, H. J., "Experimental investigation of a flat-plate closed-loop pulsating heat pipe," *Journal of Heat Transfer-Transactions of the ASME*, Vol. 141, No. 9, 2019, 091807.

[10]Feng, C., Wan, Z., Mo, H., Tang, H., Lu, L., and Tang, Y., "Heat transfer characteristics of a novel closed-loop pulsating heat pipe with a check valve," *Applied Thermal Engineering*, Vol. 141, 2018, pp. 558-564.

[11]Jung, C. and Kim S. J., "Investigation into the effects of passive check valves on the thermal performance of pulsating heat pipes," *International Journal of Heat and Mass Transfer*, Vol. 204, 2023, 123850.

[12]Ibrahim, O. T., Monroe, J. G. Thompson, S. M., Shamsaei, N., Bilheux, H., Elwany, A., and Bian, L., "An investigation of a multi-layered oscillating heat pipe additively manufactured from Ti-6Al-4V powder," *International Journal of Heat and Mass Transfer*, Vol. 108, 2017, pp. 1036-1047.

[13]Belfi, F., Iorizzo, F., Galbiati, C., and Lepore, F., "Space structures with embedded Flat Plate Pulsating Heat Pipe built by Additive Manufacturing Technology: development, test and performance analysis," *Proceedings of Joint 19th International Heat Pipe Conference and 13th International Heat Pipe Symposium*, Pisa, 2008.

[14]Maghsoudi, E., Furst B. I., Jasper, J. D., Daimaru, T., and Odagiri, K., "Efficient Thermal Management for Sampling Arm Actuators," *Proceedings of 2020 International Conference on Environmental Systems,* 2020, ICES-2020-561.

[15], Miranda, M. N., Segura, K., Dorantes, D., Hyatt, D., Olsen, R., Garner, C., McCarthy, L., Avanessian, S., Orr, R., Nakhjiri, N., Furst, B., Roberts, S., and Gayle J., "A rapid cubesat demonstration of an additive manufactured battery case with embedded oscillating heat pipes," *Proceedings of AIAA SCITECH 2023 Forum*, National Harbor and Online, 2023, AIAA 2023-1879.

[16]Ando M., Tanaka, K., Okamoto, A., Matsushige, K., Tanaka, K., and Okuma, S., "Fabrication and evaluation of ana oscillating heat pipe with check valves by metal additive manufacturing," *Proceedings of 52nd International Conference on Environmental Systems,* Calgary, 2023, ICES-2023-19.

[17] Taft, B.S., Williams A.D., and Drolen B.L., "Review of pulsating heat pipe working fluid selection," *Journal of Thermophysics and Heat Transfer*, Vol. 26, No. 4, pp.651-656, 2012.